International Journal of Environmental Science and Technology (2020) 17:161–174
https://doi.org/10.1007/s13762-019-02436-x

ORIGINAL PAPER

Microwave-assisted catalytic oxidation of methomyl pesticide by Cu/Cu_2O/CuO hybrid nanoparticles as a Fenton-like source

M. A. Tony[1,2] · **Sh. A. Mansour**[2]

Received: 12 March 2019 / Revised: 11 May 2019 / Accepted: 10 June 2019 / Published online: 15 June 2019

Abstract

Heterogeneous catalytic oxidation, Fenton-like (FL) hybrid nanoparticles (NPs) induced by microwave (MW) irradiation, was applied as a green technology pathway for methomyl pesticide oxidation. Three different hybrid nanostructured particles, C300, C400 and C500 containing various phase structures, i.e., Cu, Cu_2O and CuO, were successfully synthesized by the thermal decomposition technique and used as a FL source in microwave-induced (MW/FL) system. The microstructure and morphology of the hybrid nanostructured particles were studied using an X-ray diffraction (XRD) field-emission scanning electron microscope (FE-SEM), respectively. Also, MW/FL system was compared to MW/H_2O_2 and (MW) alone. The influence of various operating parameters, i.e., microwave irradiation time and power, initial NPs concentration, H_2O_2 concentration and pH for the three MW/FL systems, was investigated, and the optimal operating conditions were compared. The results indicated that the MW/FL process outperformed the other systems, and around 91% of methomyl was removed after only 8 min of MW irradiation for the C300-based MW/FL system under optimal conditions. Notably, the results verified that the heterogeneous MW/FL oxidation system catalyzed over the synthesized NPs reacted with the wastewater at its initial pH without adjustment, which overcomes the weakness of the homogeneous Fenton catalyst. Hence, this advantage could expand the application of this oxidation technique and thus improves the system efficiency. Finally, the catalyst showed good reusability. The success of this technique explores the possibility of copper as a non-iron FL system in a MW-assisted system for the rapid removal of methomyl from wastewater.

Keywords Copper-modified Fenton-like · Methomyl · Microwave irradiation · Wastewater · Cu nanoparticles

Introduction

Ground and surface water pollution is increasing at an unprecedented rate that certainly threatens human and aquatic systems. Generally, most water pollution occurs in ecosystems as a result of human activities. Recently, pesticides constitute one of the major groups of organic complexes that cause serious environmental challenges due to their application in significant quantities in agriculture to promote plant protection from insects, fungi and bacteria that harm the harvest. In addition, their high water solubility, chemical stability and biodegradation resistance enable them to spread to the groundwater. Consequently, novel treatment technologies to mineralize those toxic substances are urgent.

Methomyl, which belongs to the oxime carbamate family of pesticide groups, is being widely used in agriculture due to its powerful control of different types of pests and insects. However, it has a high solubility value in water (57.9 g/L, 20 °C) making it hazardous to surface and groundwater in agricultural regions (Raut-Jadhav et al. 2016). Thus, the European Commission (EC), Environmental Protection Agency, USA (EPA) and World Health Organization (WHO) classified the methomyl as a restricted, very toxic and hazardous pesticide because it is extremely toxic to the ecosystem (Malato et al. 2003; Zhang et al. 2017).

Editorial responsibility: M. Abbaspour.

✉ M. A. Tony
dr.maha.tony@gmail.com

[1] Civil and Environmental Engineering, West Virginia University, Morgantown, WV 26506-6103, USA

[2] Advanced Materials/Solar Energy and Environmental Sustainability (AMSEES) Laboratory, Basic Engineering Science Department, Faculty of Engineering, Menoufia University, Shebin El-Kom, Egypt

For decades, different conventional techniques have been applied for the mineralization of toxic water pollutants. Methomyl has been removed from wastewater by adsorption (Chang and Lee 2012; Ashour et al. 2014; Akl et al. 2016; Ashour and Tony 2017), ozonation (Mico et al. 2010), photo-Fenton reagent (Zhao et al. 2009; Mico et al. 2010) and sonication (Raut-Jadhav et al. 2016). However, the search for environmentally friendly and efficient methodologies is of growing interest.

Among conventional treatment technologies, photochemical reactions based on the powerful oxidizing ˙OH radicals species, so-called advanced oxidation processes (AOPs), are gaining a considerable attention to degrade toxic pollutants to harmless end products in an effective and economic approach (Ciesla et al. 2004). Concerning the various AOPs, the Fenton approach is considered the most popular system which is applied extensively in the treatment of several pollutants such as oily wastewater (Lucas and Peres 2009; Tony et al. 2015), dyes (Medien and Khalil 2010; Tony and Mansour 2019), humic substances, phenols (Wu et al. 2010) and launderette wastewater (Tony et al. 2016). The traditional homogenous Fenton system is based on the production of ˙OH radicals by the catalytic decomposition of H_2O_2 by $Fe^{2+/3+}$ (Wu et al. 2010; Tony et al. 2011). However, several disadvantages associated with those homogenous Fenton processes, for instance the limiting pH value (around 3), require either pre- or post-treatment of the wastewater (Tony and Bedri 2014). Moreover, the dissolved iron species in the wastewater after treatment may need post-purification that increases the overall process cost. Those homogenous Fenton process disadvantages result in limited process efficiency.

There is a great interest in using nanoparticles (NPs) for promoting the catalytic activity of chemical reactions. Synthesis and exploration of various functionalized NPs are gaining extensive attention both in academia and in industry. According to the previous investigations (Tony et al. 2018), the application of those NPs in various fields, especially in wastewater, increases the overall system efficiency. A range of synthetic strategies are available for preparing the NPs, such as ionic liquid (Zhang et al. 2015a, b), wet chemical (Gong et al. 2014), reverse micelle (Lu et al. 2010; Solanki et al. 2010), microwave-assisted (Zhu et al. 2004; Dar et al. 2012), biosynthesis (Abboud et al. 2014), electrochemical (Theivasanthi and Alagar 2011) and sonochemical (Zhang et al. 2015a, b). However, such techniques still have some limitations. Much effort has been expended in the development of cost-efficient and rapid synthesis techniques for NPs with a reasonable product yield. Challenges still exist in the widespread use of NPs at a mass production scale. These challenges include the limited yield of NPs and the cost of their preparation. Thus, to overcome these challenges, alternative synthesization techniques to obtain a high yield of production with reduced cost, such as the thermal decomposition technique (Lin and Li 2009; Sunaina et al. 2017), have been developed. Other examples include the substitution of the homogenous Fenton system with the heterogeneous one to overcome the system drawbacks. This alternative heterogeneous Fenton-like system is based on the transitional metals or metal oxides as a source of the heterogeneous catalyst (Soon and Hameed 2011). Copper-based heterogeneous Fenton-like catalysts are of prime importance due to their significant catalytic activity (Pan et al. 2015) and selectivity (Valdez et al. 2012), in addition to the fact that the reaction can be achieved around the neutral pH range (Zhong et al. 2012a, b). Additionally, Cu-based nanoparticles are specifically attractive since copper is cheap and naturally abundant (Gawande et al. 2016).

The key to the Fenton-like process is the production of the ˙OH radicals. Thus, the process could be assisted to produce higher ˙OH radicals concentration using systems such as ultraviolet light (Chen and Zhu 2007; Tony et al. 2018), ultrasonic enhancement (Raut-Jadhav et al. 2016) and microwave irradiation (Gromboni et al. 2007).

In the last few years, microwave irradiation has been widely used in areas which include domestic, medical and industrial applications due its observable heating effect. Additionally, it helps to change system thermodynamics, weaken chemical molecule bonds and reduce system activation energy, thus improving the chemical reaction kinetics (Ai et al. 2008). Such applications include pyrolysis (Menendez et al. 2002), adsorption (Hsieh et al. 2006), extraction (Abu-Samra et al. 1975) and synthesis (Cao et al. 2009). Microwave irradiation has been applied in environmental engineering applications such as soil remediation (Remya and Lin 2011), sludge and wastewater treatment (Ai et al. 2008) and chemical catalysis (Zhang and Hayward 2006). However, according to the literature, it has not been applied so far in the copper-nanocatalysis-based Fenton-like oxidation.

In the present investigation, synthesis of three categories of Cu-based nanoparticles (NPs) was examined. Microwave (MW) was introduced to increase the catalytic activity and enhance the Fenton-like (FL) system based on the Cu nanoparticles and to increase the rate of ˙OH radical production for the selective and rapid treatment of methomyl pesticide in wastewater, which is widely used in Egypt. The influence of different operating parameters was examined, and the MW technique was shown to have a positive influence on reaction kinetics. Additionally, the performance of various forms of

Cu nanoparticles when combined with MW in the MW/FL system was compared.

Materials and methods

Materials

Wastewater

Commercial-grade methomyl (S-methyl N-[(methylcarbamoyl) oxy] thioacetimidate), 90% concentration, from central agricultural pesticide and chemicals company, El-Menoufia, Egypt, was used as a model pollutant without any further purification. A stock solution of 1000 ppm was prepared, and a further dilution was done, as required to (50, 100, 200, 400 mg/L). A volume of 50 mL of aqueous methomyl solution was used in all the treatment experiments.

Catalyst and reagents

$CuO/Cu_2O/Cu$ hybrid nanostructure samples were synthesized by thermal decomposition of copper (II) acetate monohydrate, $CuAc_2{\cdot}H_2O$, in air. In a typical procedure, 3 g from $CuAc_2{\cdot}H_2O$ was introduced into a covered 50-mL alumina crucible. Thereafter, the crucible was placed in an oven for 3 h at T_d, where T_d is the selected temperature to obtain various ratios between the counterparts of the hybrid nanostructures (Obaid et al. 2000; Lin et al. 2012). The reaction product was collected after slow cooling in air overnight. The samples are labeled as C300, C400 and C500 which corresponding to different T_d at 300, 400 and 500 °C, respectively. All the T_d temperatures were selected to be sufficient for the complete thermal decomposition process as well as the time of exposure to the thermal heating (Lin et al. 2012).

Hydrogen peroxide (30% w/v) was used to initiate the Fenton-like system. Sodium hydroxide (NaOH) and sulfuric acid (H_2SO_4), all of analytical grade obtained from Sigma-Aldrich, were used for wastewater pH adjustment to the desired values.

Characterization

The phase structure of the samples obtained was examined using X-ray powder diffraction using an XRPhillips X'pert diffractometer, MPD 3040, throughout 2θ ranging from 20 to 80°. The collected diffraction intensities were recorded with step-scan mode to get the X-ray diffraction (XRD) pattern for each sample. The morphology of the investigated powder samples was characterized by field-emission scanning electron microscope (FE-SEM), Quanta FEJ20.

Methodology

MW irradiation to enhance the FL was accomplished in a household 2.45-GHz microwave oven (100–1000 W) fitted with time controller and rotating platform. Firstly, for every experiment performed, 50 mL volume of methomyl wastewater pesticide samples was placed in a container and the required amounts of the prepared nanocopper particles, namely C300, C400 or C500, were added and the FL reagent initiated by the addition of H_2O_2. The pH of solution was set at the desired values by adding required amounts of H_2SO_4 or NaOH solutions before adding the given amounts of FL reagent. Thereafter, FL was well dispersed with the methomyl solution before it was placed in the MW oven to be irradiated for the required reaction time at a certain input power level. Afterward, residual methomyl concentrations in the treated wastewater were measured. Figure 1 shows the schematic flow diagram of the Fenton-like (FL) enhanced with the microwave treatment.

Analytical determinations

Wastewater samples were taken after the reaction time in each case. The samples were filtered using a microfilter to remove the NPs. Thereafter, the residual concentration of methomyl was measured by recording the absorbance at 231 nm using a UV–visible spectrophotometer (Unico UV-2100 spectrophotometer, USA, with modification). The pH of the pesticide solution was measured using a digital pH-meter (AD1030, Adwa instrument, Hungary).

Results and discussion

XRD characterization of the synthesized $CuO/Cu_2O/Cu$ hybrid nanostructure samples

Figure 2 shows XRD patterns of the synthesized powder samples. The peaks obtained in these patterns exhibit the absence of any peak attributed to $CuAc_2{\cdot}H_2O$ or $CuAc_2$, whereas the patterns obtained refer to hybrid nanostructures based on $CuO/Cu_2O/Cu$ with different peak intensities, as shown in Fig. 2. As can be seen from this figure, the intensity of the diffracted peak of Cu decreased with increasing temperature and completely vanished in C500. However, the maximum-contained ratio of Cu_2O was found in C400. In addition, the predominant phase was CuO, with small traces from the Cu_2O phase. This finding was as expected due to the gradual oxidation process in air of Cu and Cu_2O to CuO, as reported by Lin et al. (2012).

The crystallite sizes *(D)* of the investigated phases for each sample were estimated using Scherrer's relation

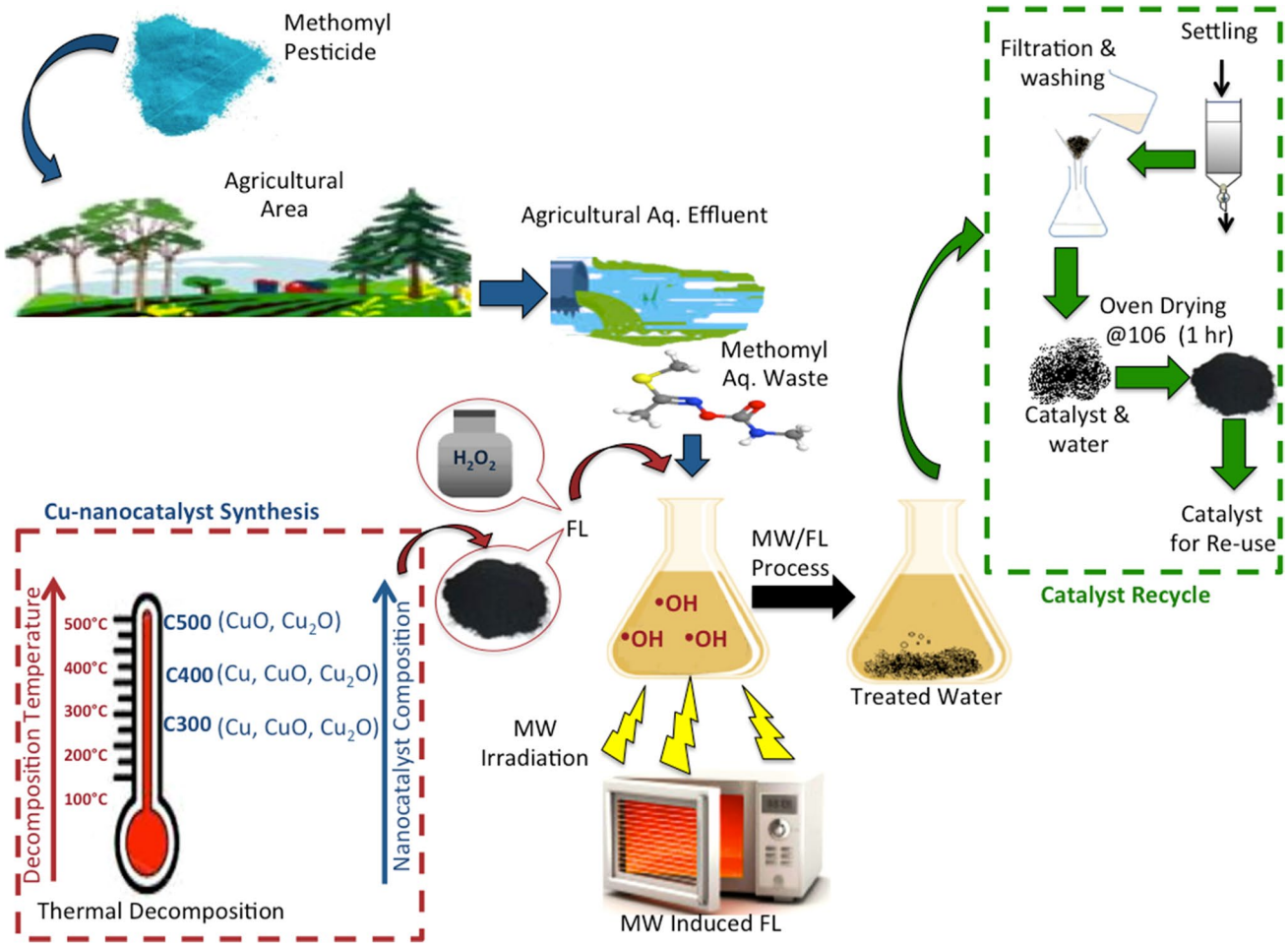

Fig. 1 Schematic representation of the experimental setup

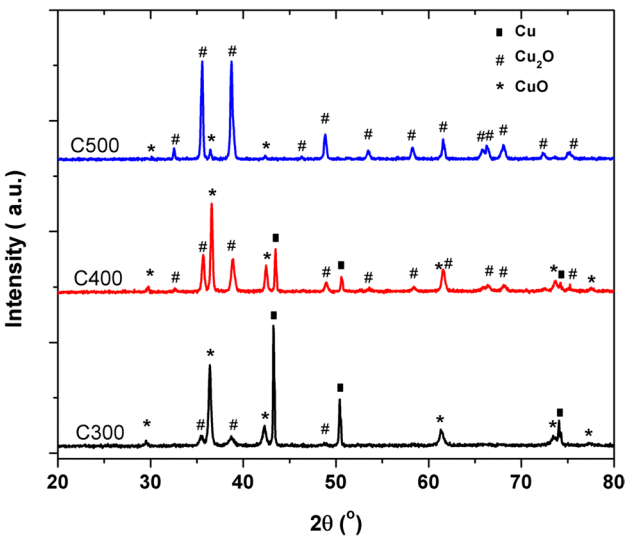

Fig. 2 XRD diffraction patterns of the synthesized CuO/Cu_2O/Cu hybrid nanostructure samples

(Scherrer 1918) to determine the most preferred plane for the phase. This plane was found to be 43.2°, 36.4° and 38.3° for Cu, Cu_2O and CuO phases, respectively. Figure 3 shows the variation of D for each phase with different T_d. The values of D obtained for all phases are less than 100 nm, which shows the formation of nanostructured particles. This figure shows the same trend for Cu_2O and CuO phases, increasing the crystallite size (D) with increasing T_d. Such a trend could be attributed to expected crystal growth of these phases with increasing temperature. It is also clear that the rate of increase of D is higher in the case of CuO phase than in the case of Cu_2O phase, especially from 400 to 500 °C. This observation can be explained by the oxidation process of Cu_2O to CuO phase at 500 °C. In respect of the D of Cu_2O to CuO phases, the Cu phase showed a reduction in D value with an increase in T_d temperature. Such differences could be attributed to the expected cessation in crystal growth of the Cu phase due to the reduction of this phase with temperature as a result of the oxidation process to CuO phase.

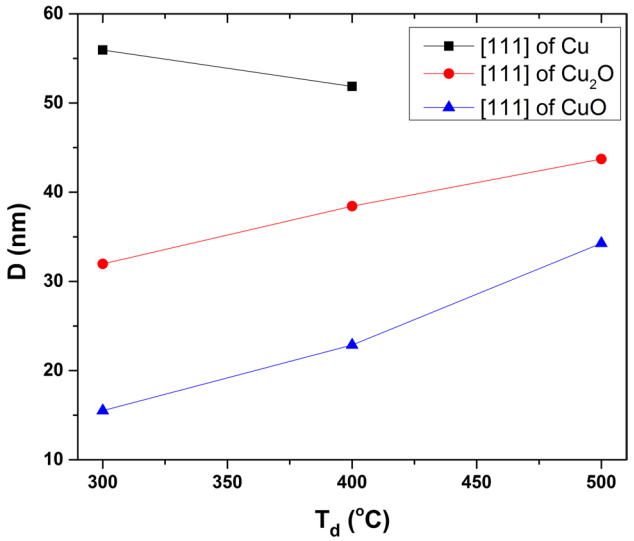

Fig. 3 The variation of crystallite size (D) of the phases at T_d temperature along the [111] plane

The maximum concentration of the Cu phase was obtained after the decomposition of $CuAc_2{\cdot}H_2O$, as reported by Lin et al. (2012).

Morphological characterization of the nanostructure samples

Figure 4 shows the FE-SEM micrographs of the synthesized powder samples. Figure 4a, b reveals a non-uniform shape of the particles obtained for C300 with some uniform hexagonal shapes (the inset of Fig. 4a), which can be referred to Cu nanoparticles (Xiong et al. 2011). However, the particles obtained of C400 and C500 exhibit agglomeration of porous particles, as shown in Fig. 4c, e, respectively. The size of such particles for C500 was higher than that obtained in C400, which confirms the role of increasing temperature in the decomposition process (T_d) with the increase in the crystal growth, as discussed previously in Sect. 3.1. Magnification of FE-SEM for samples C400 and C500 (Fig. 4d, f, respectively) showed rosette-like and gypsum rose morphology of such samples. Examination of the figure shows the uniform shape of the particles of C400 and C500, although these samples include hybrid (Cu, Cu_2O and CuO) nanostructures. This apparent contradiction could be explained by the fact that all of the hybrid phase had the same predominant plane [111], which enabled them to grow along the same orientation.

Process performance

To investigate the effect of different degradation systems for methomyl polluted wastewater removal, solo MW treatment, MW/H_2O_2, FL, C400 nanoparticles and MW/FL were conducted for methomyl degradation. The results in Fig. 5 show that the MW system alone had very little effect on methomyl removal. However, when the MW/H_2O_2 was combined with FL processes, a considerable improvement was observed. In addition, the C400 addition alone had no effect on the methomyl degradation. The combined use of FL and MW, i.e., MW/FL system, achieved the highest removal efficiency of methomyl, which exceeded 89%. This reflects the effectiveness of MW/FL as an alternative removal method for methomyl pesticide.

Comparing the results, the order of methomyl removal is: MW/FL > MW. No removal for Cu-based system was observed and a negligible effect for Mw/H_2O_2 and FL systems. H_2O_2 reagent addition caused a negative impact on the methomyl pesticide degradation. This finding has previously been found by Tony et al. (2008), that hydrogen peroxide alone is not effective due to its low reaction rate.

This series of experiments illustrated the synergistic effect of MW/FL technique in degrading the methomyl pesticide. Clearly, in the MW/FL reaction concerning the C400 ions combined with H_2O_2 generates $^{\cdot}OH$ radicals that played an important role in the methomyl degradation. As previously stated in the literature (Fernández-Alba et al. 2002; Malato et al. 2002; Malato et al. 2003; Tamimi et al. 2006; Oller et al. 2006; Tamimi et al. 2008), methomyl molecules decompose completely into CO_2, H_2O, NO_3^- and SO_4^- when the pesticide is oxidized by TiO_2 or photo-Fenton process. Thus, MW/FL oxidation of methomyl is an environmentally friendly system for pesticide removal.

Effect of various MW/FL parameters

Effect of methomyl concentration

The initial methomyl pesticide concentration effect on the MW/FL catalyzed with C400 degradation technique was examined at various methomyl concentrations, and the results are shown in Fig. 6. It is clear from the observed results that, as the initial methomyl concentration increased from 50 to 100 mg/L, the methomyl removal efficiency decreased from 89% to 9%. However, no degradation occurred with a further increase in the initial methomyl to 1000 mg/L.

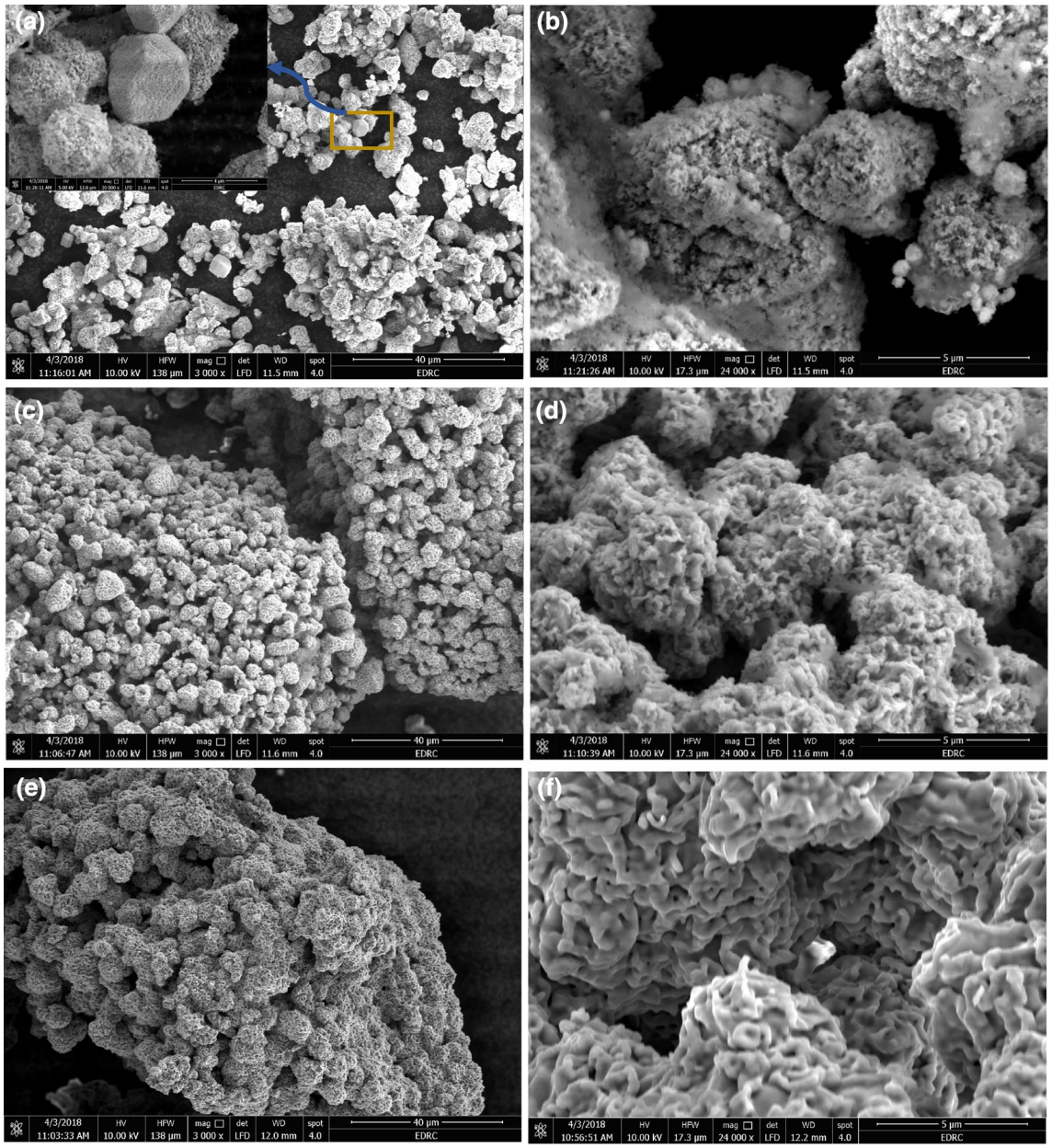

Fig. 4 FE-SEM micrograph images of the synthesized hybrid nanostructure samples: **a**, **b** C300, **c**, **d** C400 and **e**, f C500

The above observation can be explained by the relationship between the concentration of ˙OH radicals produced in the system and the concentration of methomyl present in the aqueous solution. ˙OH, which is mainly responsible for the degradation of methomyl, is produced to a certain concentration in the system. Thus, at a constant ˙OH concentration, the increase in the methomyl concentration decreases the relative radical concentration, and hence, the overall efficiency is retarded. However, at initial methomyl concentrations in the range from 200 to 1000 mg/L, the radicals could not degrade the methomyl pollutant as more molecules of methomyl are available for degradation. This observation is in accordance with the previous findings of Kalal et al. (2015) using trypan blue dye in a heterogeneous Fenton system.

Effect of irradiation time and power

The objective of this series of experiments was to select the best operational conditions in the MW/FL system. The dosage of H_2O_2 and Cu-NPs was 5000 mg/L and 3.0 g/L, respectively, and the pH was kept at 6.5 (without adjustment). Firstly, the microwave power was set at 500 W to

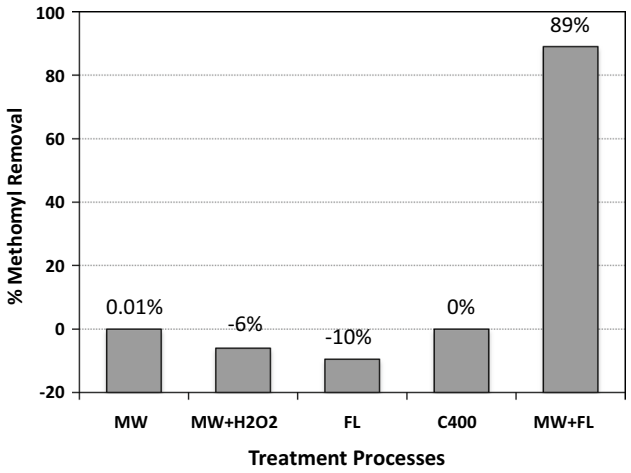

Fig. 5 Effect of the treatment systems

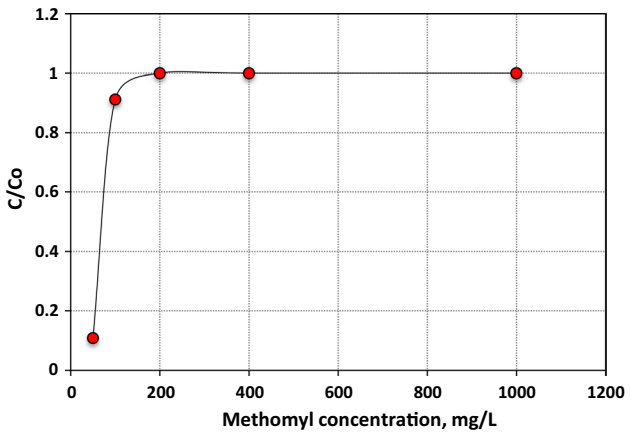

Fig. 6 Effect of initial methomyl concentration on MW/FL catalyzed with C400 NPs (MW power 500 W; irradiation time 5 min; H_2O_2 concentration 5000 mg/L; pH 6.5)

investigate the optimum MW irradiation time for all Cu-based NPs systems, namely C300, C400 and C500.

Figure 7 shows that for 500 W microwave power the irradiation time improves the methomyl removal rate for the C300/, C400/and C500/H_2O_2 systems. However, the optimal irradiation time differs in the three systems. For the MW/FL system based on C300 NPs, the maximum methomyl removal was 83% for 8.0 min of reaction time, while C400 and C500 NPs achieved a maximum 89 and 16%, at 5 and 12 min of MW irradiation time, respectively. Under a constant MW energy utilization, oxidation requires reaction times dependent on the catalyst used. This means that the lower the MW power, the long the irradiation time to complete the methomyl removal. Thus, the removal efficiency, as shown in Fig. 7, increased with extending the irradiation time at a constant MW energy consumption. This result agrees with Iboukhoulef et al. (2013) who investigated 5 min of irradiation time in microwave-assisted Fenton-like system for treating phenolic compounds. The optimal irradiation time for each NP was subsequently selected for the further investigations.

Since MW energy is a controlling parameter in the MW-induced systems, different MW power sources (200–800 W) were studied. Figure 8 shows that methomyl removal rate can be improved by an increase in the MW power, in particular for the MW power ranging from 400 to 500 W. However, FL reaction induced slowly at lower or higher MW energy. The reaction between Cu-based NPs and H_2O_2 in the FL system generates maximum ˙OH radicals when it is exposed to a higher MW energy. This phenomenon is explained by the fact that MW energy induces a motion of the H_2O_2 molecules, which therefore increases the collision numbers. Moreover, the peroxide molecules are raised to a higher excited state, including greater vibrational and rotational energy levels. Thus, the result has weakened in the molecular bonds and subsequently split (Homem et al. 2013). Furthermore, hotspots may develop because of the superheating induced by the MW energy at a high temperature on the surface of Cu-based NPs catalyst induced by the Maxwell–Wagner effect of microwaves (Ai et al. 2008). Hence, the existence of such hotspots accelerates the reaction of hydrogen peroxide and methomyl molecules, attacked by the Cu-based catalyst.

The MW irradiation time and power correlate with the methomyl removal efficiency as they are dependent on ˙OH radicals and H_2O_2 decomposition. The results show that the methomyl residual decreases with an increase in MW power and time up to a certain limit. The optimal MW power energy of 500 W (for C400 NPs) and 400 W (for C300 and C500 NPs) was thus used in subsequent experiments.

Effect of amount of H_2O_2

The hydrogen peroxide dose is considered an important parameter in the FL reaction since the oxidation in the MW/FL process is based on the concentration of ˙OH produced. The data presented in Fig. 9 show that methomyl removal marginally increases with increasing H_2O_2 for the three copper-catalyzed systems (C300, C400 and C500). A significant enhancement is observed for methomyl removal at a H_2O_2 dose of 5000 mg/L. This phenomenon may be due to the fact that ˙OH radicals that are mainly responsible for the methomyl oxidation are produced through H_2O_2 decomposition under microwave irradiation, as shown in Eq. (1) (Pan et al. 2015). Furthermore, the reaction between CuO or Cu_2O and H_2O_2 results in more ˙OH radical production that attacks the chemical bonds in methomyl molecules (Eqs. 2, 3). Consequently, this leads to the formation of reaction intermediates

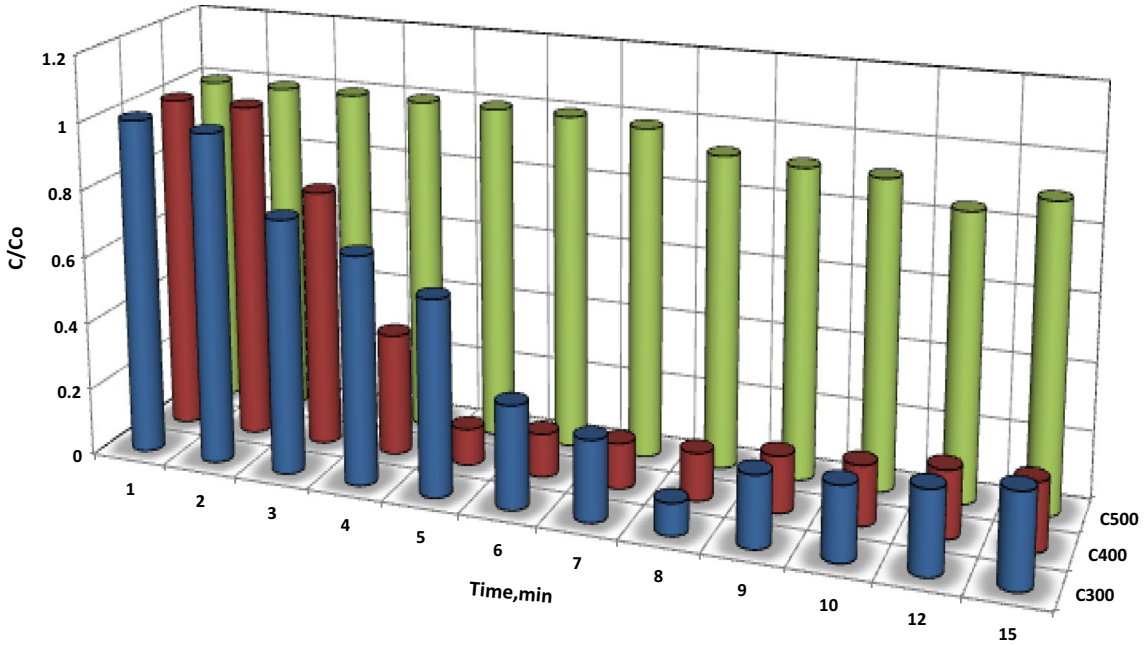

Fig. 7 Effect of microwave irradiation time on the methomyl removal in MW/FL reaction (MW power 500 W; initial methomyl concentration 50 ppm; initial H_2O_2 concentration 5000 mg/L; pH 6.5)

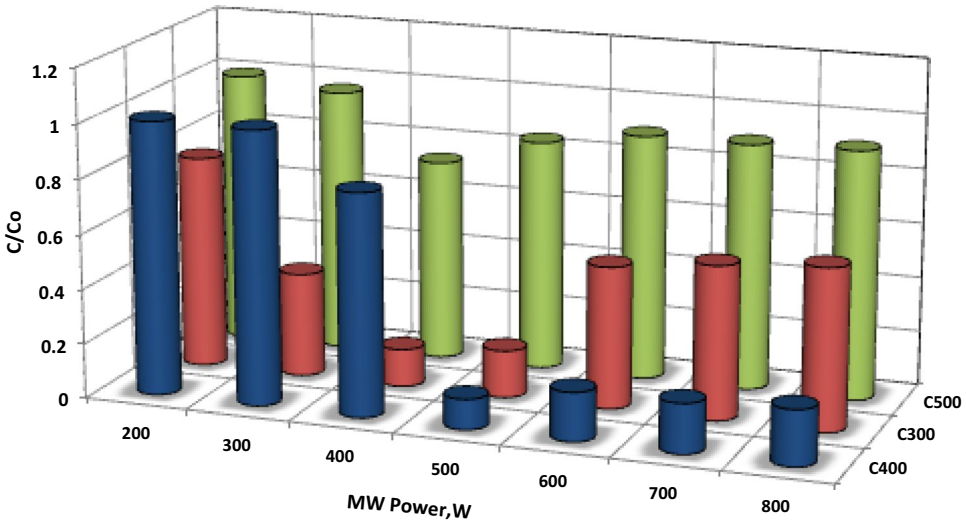

Fig. 8 Microwave power effect on methomyl removal in MW/FL reaction (irradiation time 5 min; initial methomyl concentration 50 ppm; initial H_2O_2 concentration 5000 mg/L; pH 6.5)

that are eliminated by additional ˙OH species, resulting in the final end product formation of H_2O and CO_2 (Zhong et al. 2012a, b).

$$H_2O_2 + \text{MW energy} \rightarrow 2\,{}^{\cdot}OH \quad (1)$$

$$Cu^{2+} + H_2O_2 \rightarrow Cu^{+} + HO_2^{\cdot} + H^{+} \quad (2)$$

$$Cu^{+} + H_2O_2 \rightarrow Cu^{2+} + {}^{\cdot}OH + OH^{-} \quad (3)$$

A further increase in the H_2O_2 peroxide dose did not result in a greater conversion of methomyl yield. This finding could be explained by the fact that, at high H_2O_2 concentrations, the peroxide acts as an ˙OH radical scavenger, instead of producing them as illustrated in Eqs. (4) and (5) (Neamtu et al. 2002; Ramirez et al. 2007). In addition, re-combination reaction of ˙OH radicals producing H_2O_2 occurred contributing further to ˙OH radical scavenging capacity (Eq. (6)) (Tamimi et al. 2008).

$$H_2O_2 + HO^{\cdot} \rightarrow HO_2^{\cdot} + H_2O \quad (4)$$

$$HO_2^{\cdot} + HO^{\cdot} \rightarrow H_2O + O_2 \quad (5)$$

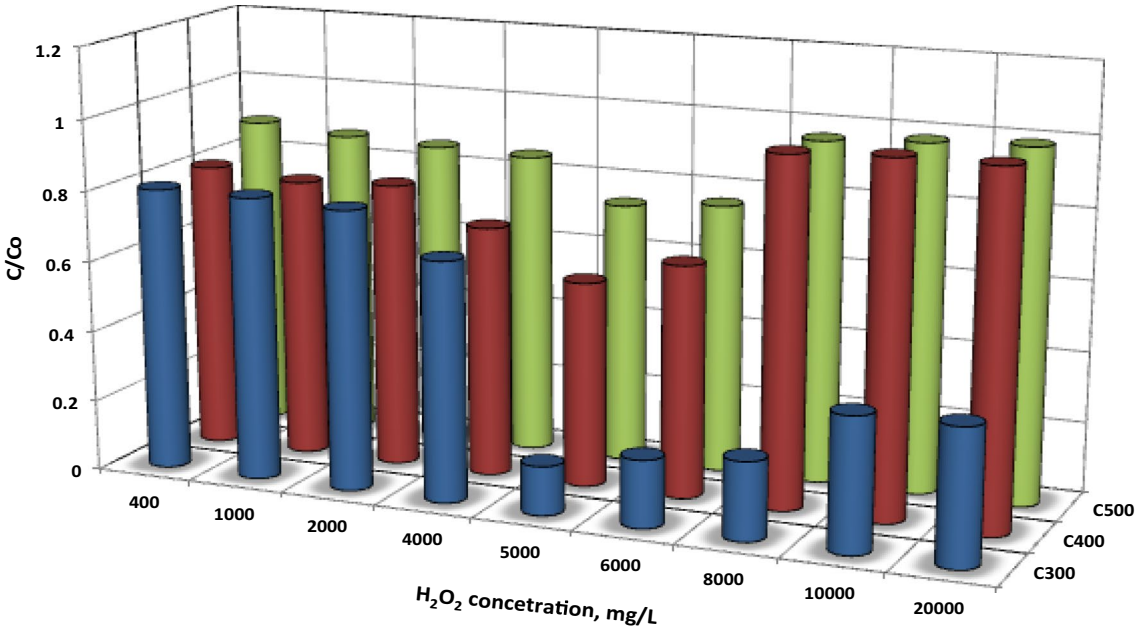

Fig. 9 Effect of initial H_2O_2 on methomyl removal (initial methomyl concentration 50 ppm; pH 6.5; catalyst dosage 3.0 g/L)

$$HO^{\cdot} + HO^{\cdot} \rightarrow H_2O_2 \quad (6)$$

A similar trend showing an increase in the reaction rate with increasing peroxide concentration is evident for the copper-based catalysts up to a certain limit when the reaction rate decreased, C300 NPs resulting in higher methomyl removal rate compared to C400 and C500, 91%, 89 and 26%, respectively. It could be observed from the XRD results presented in Fig. 3 that copper oxides (Cu_2O, CuO) and metallic copper were present in C300 and C400 NPs and copper oxides only in C500 NPs. As shown in Eqs. (2, 3), Cu^+ activates H_2O_2 which is not responsible for the direct $^{\cdot}OH$ radicals formation, but is involved in the production of a higher oxidation state of copper, so-called Cu^{2+}. Those existed in a lower reaction rate compared to the strong oxidizing species $^{\cdot}OH$ radical which are non-selective. Thus, these radicals are competing with $^{\cdot}OH$ radicals in methomyl oxidation.

Hence, hydrogen peroxide should be added to enhance the FL reaction at an optimum dose to achieve the best removal efficiency. Therefore, 5000 mg/L is considered the optimum value for all MW/FL applied in this study.

Cu-based NPs loading

Figure 10 illustrates the effect of different NP catalyst dosages (C300, C400 and C500) on methomyl removal. It is clear from the results that, for all the Cu-based NP systems, the methomyl removal is greatly enhanced by the NPs concentration increasing from 0.01 to 3 g/L. However, beyond this dose, the methomyl oxidation rate declines with a further increase in the concentration of NPs catalyst, saturation being reached. Generally, at higher NPs catalyst value, more active sites are generated which may accelerate the production of hydroxyl radicals ($^{\cdot}OH$). Thus, this promotes the overall methomyl removal efficiency (Pan et al. 2015; Tony et al. 2016). Nevertheless, beyond this certain limit, further increase in the NPs catalyst dose results in a retardation of the reaction. This change in the removal rate occurred due to the fact that, at a constant concentration of H_2O_2, the amount of this peroxide reagent is not enough to be decomposed by NPs catalyst. Therefore, the relative $^{\cdot}OH$ radicals concentration declined, leading to a decrease in the overall methomyl removal. Hence, it can be concluded that the optimum NPs catalyst dosage for all the systems under the present MW/FL study was 3.0 g and the removal efficiency was 91% for C300 NPs system. This performance is similar to other studies reported by Bradu et al. (2010), Valdez et al. (2012) and Pan et al. (2015).

Although similar results were observed for the three Cu-based catalysts (C300, C400 and C500), that is, increasing the dose of NPs catalyst improves the methomyl removal rate, it is clear from Fig. 7 that C300 and C400 are more sensitive to the catalyst dose and the overall efficiency is high at around 90% compared to only 26% when C500 is used. Generally, the catalytic activity of Cu_2O is higher than that of CuO that generates higher $^{\cdot}OH$ that attacks the organic pollutants. CuO particles are inadequate to initiate

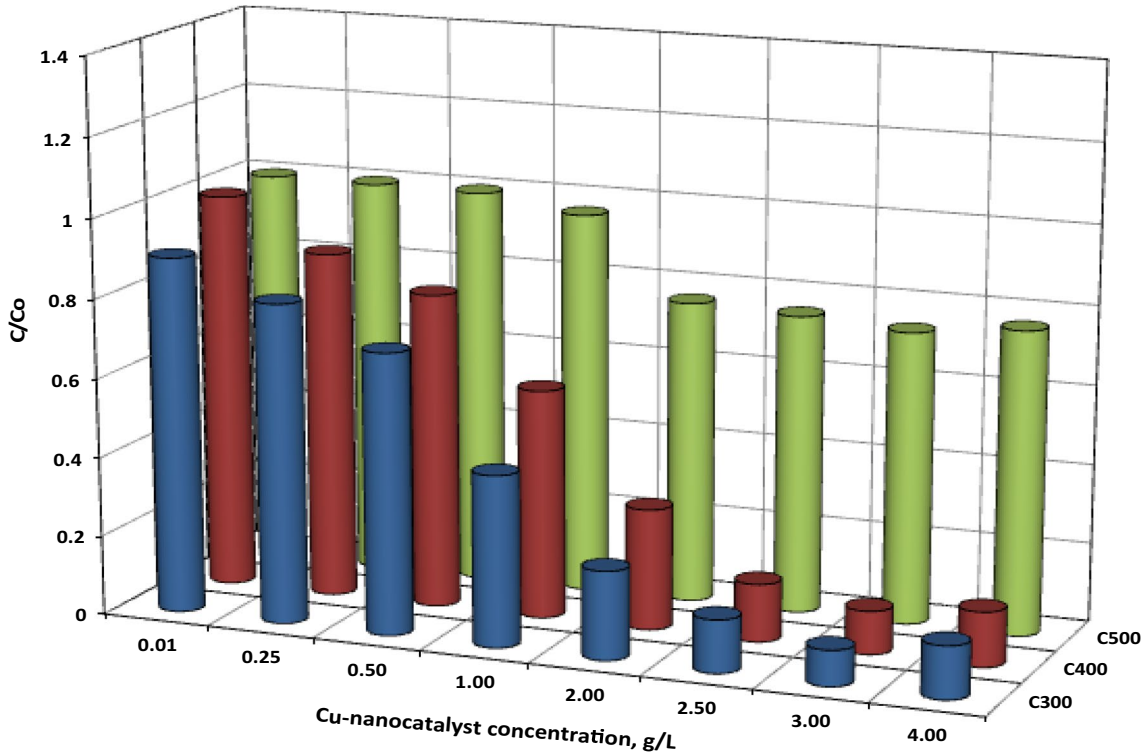

Fig. 10 Effect of initial Cu-based NPs load on methomyl removal (methomyl initial concentration 50 ppm; pH 6.5; catalyst dosage 3.0 g/L)

the ˙OH and superoxide radical that are both considered as primary initiators for the oxidation process. Therefore, the combination of CuO/Cu_2O NPs is recommended. Thus, as discussed in XRD results the decomposition temperature of Cu-based NPs formation increases from 300 to 500 °C, with a steady decrease in metallic Cu and Cu_2O oxide and a gradual increase in CuO oxide formation. This indicates the conversion of Cu to CuO with a small amount of Cu_2O present in C500. Thus, the result is a reduction in the overall methomyl removal rate (Janczarek and Kowalska 2017; Lin et al. 2012). Furthermore, metallic Cu form in C300 and C400 NPs, under the MW irradiation,

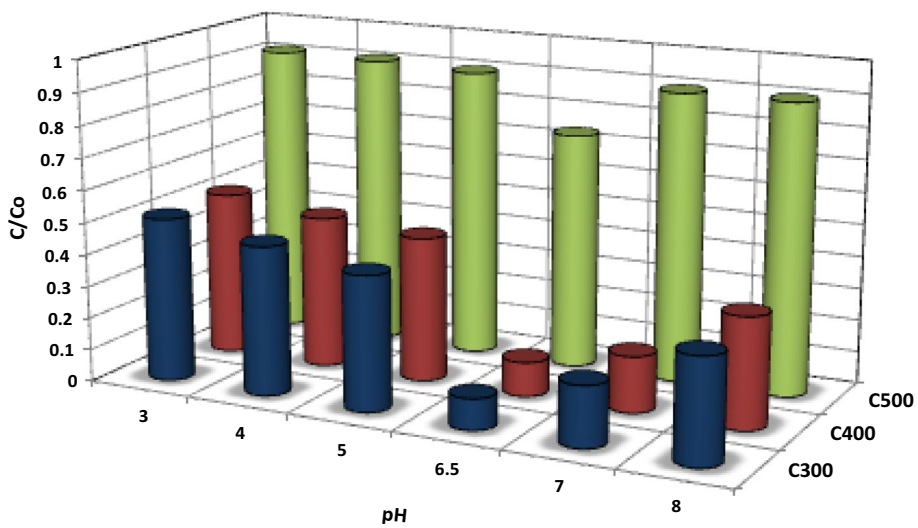

Fig. 11 Effect of initial pH on methomyl removal (initial methomyl concentration 50 ppm; H_2O_2 dosage 5000 mg/L; catalyst dosage 3.0 g/L)

is oxidized to Cu_2O. Thus, the amount of Cu_2O increases which increases the ˙OH radicals' yield. However, in the case of C500 no metallic copper is present and the amount of ˙OH radicals is less than that produced through C300 and C400 systems.

Effect of initial pH value

As previously stated in the literature (Hu et al. 2011), the oxidation process via conventional Fenton process is significantly influenced by the pH of the reaction environment. The reactions are maximized at the optimum pH value, and maximum degradation is achieved when the solution pH is around 3.0.

To examine the effect of pH in MW/FL system based on Cu-based NPs, the wastewater pH was adjusted before the MW/FL catalytic reaction reached the desired values. As presented in Fig. 11, the pH was investigated in the range 3.0–8.0 for three copper catalyst (C300, C400 and C500) systems. For the purpose of comparison, the microwave power and irradiation time were set at the optimum conditions in each copper-catalyzed system, as aforementioned. It was observed that, for the three systems, there was a slight increase in the methomyl removal rate with an increase in pH and the maximum removal was attained at the original aqueous methomyl pH (6.5). However, further increase in pH decreased the reaction rate. The pH value of the wastewater affects the decomposition of H_2O_2. Consequently, a greater concentration of ˙OH radicals is generated at higher pH. A further increase in pH above 6.5 results in more hydroxyl ions being generated and adsorbed by the catalyst instead of generating ˙OH radicals. This results in the removal rate of methomyl decreasing. This observation of increasing the removal rate around pH 6.0 is similar to that previously reported by Lee et al. (2013) in the oxidation of phenol by Cu(II)/H_2O_2 system and Kalal et al. (2015) in dye degradation using copper as a photo-Fenton-like catalyst.

The removal of methomyl in a copper-catalyzed MW/FL system attained 91, 89 and 26% removal for C300, C400 and C500 catalyzed systems, respectively, when the initial pH of the aqueous solution was 6.5 (without adjustment). This finding expands the application of the system since the reaction is independent of the acidic pH (around 3.0), as is generally the case in conventional Fenton (-like) systems (Malik and Saha 2003; Tony and Bedri 2014).

Catalyst reusability

An importance feature of this investigation is the reusability of the NPs. For catalyst re-generation, NPs were collected after each cycle and subsequently filtered before it was subjected to three sequential washings with distilled water and then dried at 110 °C for 1 h. Successive cycles after MW-induced Cu-based NPs for methomyl treatment were monitored for the pesticide removal efficiency, and the results are shown in Fig. 12.

As illustrated in the figure, upon multiple uses, the catalytic activity of the NPs catalyst decreased. For C300 NPs, the performance ranged from 91% (in the fresh use) to 56% (after the sixth cycle). Thus, this could be attributed to the C300 NPs (Cu, CuO and Cu_2O) active sites which may have been occupied by some organic intermediates that covered those active centers preventing them from attacking the organic pollutants. Therefore, the overall reaction rate decreased (Bradu et al. 2010; Pan et al. 2015).

A significant decline in the methomyl removal efficiency using C400 NPs after the first catalyst cycle was observed

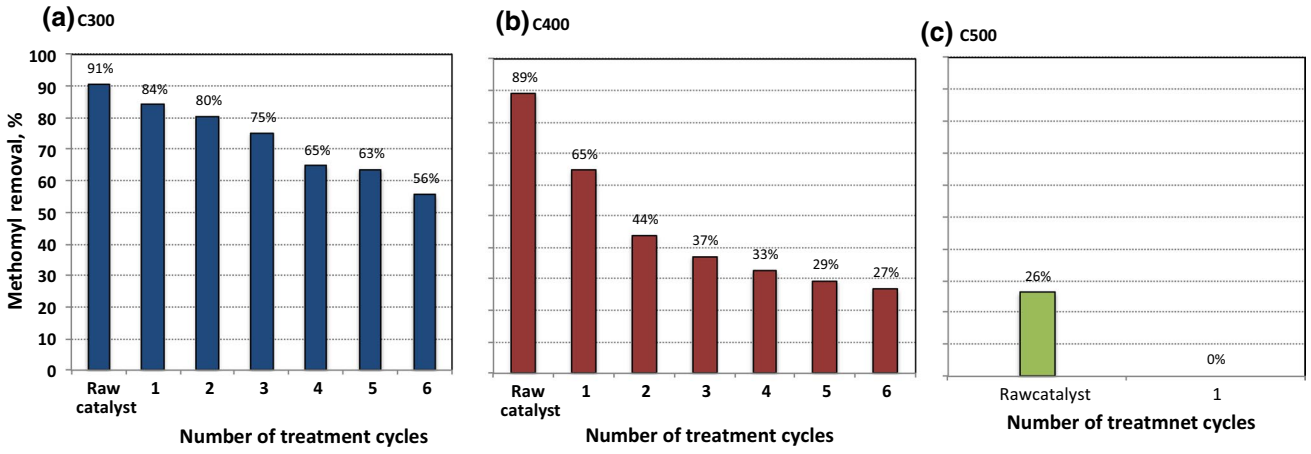

Fig. 12 Methomyl oxidation in MW/FL system in consecutive cycles (initial methomyl concentration 50 ppm; H_2O_2 5000 mg/L; catalyst dose 3.0 g/L; pH 6.5)

(65%), reducing to only 27% after the sixth cycle compared to 56% when C300 was used for treatment at the same conditions. For C500, no degradation occurred beyond the first cycle (results are not shown).

As discussed above, NPs were separated from the water samples after treatment to check the remaining methomyl and the concentration of catalyst recycled. Although the objective was to recycle all NPs in the solution, inevitably some catalyst was lost. NPs concentration after each reaction was determined, and the copper loss after each cycle was estimated to be 1.4%.

Conclusion

The application of a microwave technique to the treatment of methomyl wastewater is a novel catalytic oxidation system. Different types of Cu-based nanoparticles were synthesized using a thermal decomposition technique and applied to the removal of methomyl in the MW/FL system. The results show that the presence of CuO, Cu_2O and Cu is desirable, which were oxidized and increased the ·OH radical generation. However, the maximum methomyl removal was achieved when C300 was used as a source of NPs for a FL source catalyzed by MW irradiation, achieving 91% within only 8 min. The optimum parameters were 5000 mg/L H_2O_2, C300 dose 3.0 g/L, MW power 400 W at the initial pH of 6.5 without adjustment. The results indicated the role of the MW irradiation in enhancing the generation of OH radicals. Also, the results showed the good reusability of the catalyst after several cycles. Notably, this heterogeneous system is preferred as it is overcome the drawback of the homogenous FL reaction which is limited by the initial pH of the system, thus widening the process application.

Acknowledgements The authors wish to thank all who assisted in conducting this work.

References

Abboud Y, Saffaj T, Chagraoui A, El Bouari A, Brouzi K, Tanane O, Ihssane B (2014) Biosynthesis, characterization and antimicrobial activity of copper oxide nanoparticles (CONPs) produced using brown alga extract (*Bif urcaria bif urcata*). Appl Nanosci 4:571–576

Abu-Samra A, Morris JS, Koirtyo SR (1975) Wet ashing of some biological samples in a microwave oven. Anal Chem 47(8):1475–1477

Ai Z, Wang Y, Xiao M, Zhang L, Qiu J (2008) Microwave-induced catalytic oxidation of RhB by a nanocomposite of Fe@Fe2O3 core-shell nanowires and carbon nanotubes. J Phys Chem C 112:9847–9853

Akl MA, Youssef AM, Hassan AH, Maher H (2016) Synthesis, characterization and evaluation of peanut shells-derived activated carbons for removal of methomyl from aqueous solutions. J Environ Anal Toxicol 6(2):352

Ashour EA, Tony MA (2017) Equilibrium and kinetic studies on biosorption of iron (II) and iron (III) ions onto eggshell powder from aqueous solution. Appl Eng 1(3):65–73

Ashour EA, Tony MA, Purcell PJ (2014) Use of agriculture-based waste for basic dye sorption from aqueous solution: kinetics and isotherm studies. Am J Chem Eng 2(6):92–98

Bradu C, Frunza L, Mihalche N, Avramescu S, Neat M, Udrea I (2010) Removal of reactive black 5 azo dye from aqueous solutions by catalytic oxidation using CuO/Al_2O_3 and NiO/Al_2O_3. Appl Catal B 96(3–4):548–556

Cao Y, Wei JH, Xia Z (2009) Advances in microwave assisted synthesis of ordered mesoporous materials. Trans Nonferr Metal Soc 19:656–664

Chang CF, Lee SC (2012) Adsorption behavior of pesticide methomyl on activated carbon in a high gravity rotating packed bed reactor. Water Res 46:2869–2880

Chen JX, Zhu LZ (2007) UV-Fenton discolouration and mineralization of Orange II over hydroxyl-Fe-pillared bentonite. J Photochem Photobiol A 188(1):56–64

Ciesla P, Kocot P, Mytych P, Stasicka Z (2004) Homogeneous photocatalysis by transition metal complexes in the environment. J Mol Catal A 224:17–33

Dar MI, Sampath S, Shivashankar SA (2012) Microwave-assisted, surfactant-free synthesis of air-stable copper nanostructures and their SERS study. J Mater Chem 22:22418–22423

Fernández-Alba A, Hernando D, Agüera A, Cáceres J, Malato S (2002) Toxicity assays: a way for evaluating AOPs efficiency. Water Res 36(17):4255–4262

Gawande MB, Goswami A, Felpin F, Asefa T, Huang X, Silva R, Zou X, Zboril R, Varma RS (2016) Cu and Cu-based nanoparticles: synthesis and applications in catalysis. Chem Rev 116:3722–3811

Gong MX, Fu GT, Chen Y, Tang YW, Lu TH (2014) Autocatalysis and selective oxidative etching induced synthesis of platinum-copper bimetallic alloy nanodendrites electrocatalysts. ACS Appl Mater Interfaces 6:7301–7308

Gromboni CF, Kamogaw MY, Ferreira AG, Nobrega JA, Nogueira AA (2007) Microwave-assisted photo-Fenton decomposition of chlorfenvinphos and cypermethrin in residual water. J Photochem Photobiol A 185:32–37

Homem V, Alves A, Santos L (2013) Microwave-assisted Fenton's oxidation of amoxicillin. Chem Eng J 220:35–44

Hsieh CH, Lo SL, Kuan WH, Chen CL (2006) Adsorption of copper ions onto microwave stabilized heavy metal sludge. J Hazard Mater B 136:338–344

Hu LX, Yang XP, Dang ST (2011) An easily recyclable Co/SBA-15 catalyst: heterogeneous activation of peroxymonosulfate for the degradation of phenol in water. Appl Catal B 102(1–2):19–26

Iboukhoulef H, Amrane A, Kadi H (2013) Microwave-enhanced Fenton-like system, $Cu(II)/H_2O_2$, for olive mill wastewater treatment. Environ Technol 34(7):853–860

Janczarek M, Kowalska E (2017) On the origin of enhanced photocatalytic activity of copper-modified titania in the oxidative reaction systems. Catalysts 7:317–343

Kalal S, Chanderia K, Meghwal K, Chouhan N, Ameta R, Punjabi BP (2015) Degradation of trypan blue dye using copper pyrovanadate as heterogeneous photo-Fenton like catalyst. Indian J Chem Technol 22:148–154

Lee H, Lee H, Sedlak D, Lee C (2013) pH-Dependent reactivity of oxidants formed by iron and copper-catalyzed decomposition of hydrogen peroxide. Chemosphere 92:652–658

Lin C, Li Y (2009) Synthesis of ZnO nanowires by thermal decomposition of zinc acetate dihydrate. Mater Chem Phys 113:334–337

Lin Z, Han D, Li S (2012) Study on thermal decomposition of copper(II) acetate monohydrate in air. J Therm Anal Calorim 107:1572–8943

Lu CH, Lee CH, Wu CH (2010) Microemulsion-mediated solvothermal synthesis of copper indium diselenide powders. Sol Energy Mater Sol Cells 94:1622–1626

Lucas MS, Peres JA (2009) Removal of COD from olive mill wastewater by Fenton's reagent: kinetic study. J Hazard Mater 168(2–3):1253–1259

Malato S, Blanco J, Cáceres J, Fernández-Alba A, Agüera A, Rodríguez A (2002) Photocatalytic treatment of water-soluble pesticides by photo-Fenton and TiO_2 using solar energy. Catal Today 76(2–4):209–220

Malato S, Blanco J, Vidal A, Alarcon D, Maldonado MI, Cáceres J, Gernjak W (2003) Applied studies in solar photocatalytic detoxification: an overview. Sol Energy 75(4):329–336

Malik PK, Saha SK (2003) Oxidation of direct dyes with hydrogen peroxide using ferrous ion as catalyst. Sep Purif Technol 31(3):241–250

Medien MA, Khalil SE (2010) Kinetics of the oxidative decolorization of some organic dyes utilizing Fenton-like reaction in water. J King Saud Univ (Sci) 22:147–153

Menendez JA, Inguanzo M, Pis JJ (2002) Microwave-induced pyrolysis of sewage sludge. Water Res 36:3261–3264

Mico MM, Chourdaki S, Bacardit J, Sans C (2010) Comparison between ozonation and photo-fenton processes for pesticide methomyl removal in advanced greenhouses. Ozone Sci Eng 32:259–264

Neamtu M, Siminiceanu I, Yediler A, Kettrup A (2002) Kinetics of decolorization and mineralization of reaction azo dyes in aqueous solution by the UV/H_2O_2 oxidation. Dyes Pigments 53:93–99

Obaid AY, Alyoubi AO, Samarkandy AA, Al-Thabaiti AS, Al-Juaid SS, El-Bellihi AA, Deifallah EM (2000) Kinetics of thermal decomposition of copper(II) acetate monohydrate. J Therm Anal Calorim 61:985–994

Oller I, Gernjak W, Maldonado M, Pérez-Estrada L, Sánchez-Pérez J, Malato S (2006) Solar photocatalytic degradation of some hazardous water-soluble pesticides at pilot-plant scale. J Hazard Mater 138(3):507–517

Pan W, Zhang G, Zheng T, Wang P (2015) Degradation of p-nitrophenol using CuO/Al_2O_3 as a Fenton-like catalyst under microwave irradiation. RSC Adv 5:27043–27051

Ramirez JH, Maldonado-Hódar FJ, Pérez-Cadenas AF, Moreno-Castilla C, Costa CA, Madeira LM (2007) Azo-dye orange II degradation by heterogeneous Fenton-like reaction using carbon-Fe catalysts. Appl Catal B 75:312–323

Raut-Jadhav S, Pinjari DV, Saini DR, Sonawane SH, Pandit AB (2016) Intensification of degradation of methomyl (carbamate group pesticide) by using the combination of ultrasonic cavitation and process intensifying additives. Ultrason Sonochem 31:135–142

Remya J, Lin G (2011) Current status of microwave application in wastewater treatment–A review. Chem Eng J 166:797–813

Scherrer P (1918) Bestimmung der Grösseundderinneren Struktur von Kolloidteilchen mittels Röntgenstrahlen. Nachr Ges Wiss Göttingen 26:98–100

Solanki JN, Sengupta R, Murthy ZVP (2010) Synthesis of copper sulphide and copper nanoparticles with microemulsion method. Solid State Sci 12:1560–1566

Soon AN, Hameed BH (2011) Heterogeneous catalytic treatment of synthetic dyes in aqueous media using Fenton and photo-assisted Fenton process. Desalination 269(1–3):1–16

Sunaina M, Ghosh S, Mehta SK, Ganguli AK, Jha M (2017) Investigation of the growth mechanism of the formation of ZnO nanorods by thermal decomposition of zinc acetate and their field emission properties. Cryst Eng Commun 19:2264–2270

Tamimi M, Qourzal S, Assabbane A, Chovelon JM, Ferronato C, Ait-Ichou Y (2006) Photocatalytic degradation of pesticide methomyl: determination of the reaction pathway and identification of intermediate products. Photochem Photobiol Sci 5(5):477–482

Tamimi M, Qourzal S, Barka N, Assabbane A, Ait-Ichou Y (2008) Methomyl degradation in aqueous solutions by Fenton's reagent and the photo-Fenton system. Sep Purif Technol 61(1):103–108

Theivasanthi T, Alagar M (2011) Nano sized copper particles by electrolytic synthesis and characterizations. Int J Phys Sci 6:3662–3671

Tony MA, Bedri Z (2014) Experimental design of photo-Fenton reactions for the treatment of car wash wastewater effluents by response surface methodological analysis. Adv Environ Chem 2014:1–8

Tony MA, Mansour SA (2019) Removal of the commercial reactive dye Procion Blue MX-7RX from real textile wastewater using the synthesized Fe_2O_3 nanoparticles at different particle sizes as a source of Fenton's reagent. Nanoscale Adv 1:1362–1371

Tony MA, Zhao YQ, Fu JF, Tayeb AM (2008) Conditioning of aluminium-based water treatment sludge with Fenton's reagent: effectiveness and optimising study to improve dewaterability. Chemosphere 72:673–677

Tony MA, Zhao YQ, El-Sherbiny MF (2011) Fenton and Fenton-like AOPs for alum sludge conditioning: effectiveness comparison with different Fe^{2+} and Fe^{3+} salts. Chem Eng Commun 198(3):442–452

Tony MA, Purcell PJ, Zhao YQ, Tayeb AM, El-Sherbiny MF (2015) Kinetic modeling of diesel oil wastewater degradation using the photo-Fenton process. Environ Eng Manag J 14(1):11–16

Tony MA, Parker HL, Clark JH (2016) Treatment of laundrette wastewater using Starbon and Fenton's reagent. J Environ Sci Health A 51(11):974–979

Tony MA, Parker HL, Clark JH (2018) Evaluating Algibon adsorbent and adsorption kinetics for launderette water treatment: towards sustainable water management. Water Environ J. https://doi.org/10.1111/wej.12412

Valdez HCA, Jimenez GG, Granados SG, Leon CP (2012) Degradation of paracetamol by advance oxidation processes using modified reticulated vitreous carbon electrodes with TiO_2 and $CuO/TiO_2/Al_2O_3$. Chemosphere 89:1195–1201

Wu Y, Zhou S, Qin F, Zheng K, Ye X (2010) Modeling the oxidation kinetics of Fenton's process on the degradation of humic acid. J Hazard Mater 179(1–3):533–539

Xiong J, Wang Y, Xue Q, Wu X (2011) Synthesis of highly stable dispersions of nanosized copper particles using L-ascorbic acid. Green Chem 13:900–904

Zhang X, Hayward DO (2006) Applications of microwave dielectric heating in environment-related heterogeneous gas-phase catalytic systems. Inorg Chim Acta 359:3421–3433

Zhang B, Yuan Y, Philippot K, Yan N (2015a) Ag-Pd and CuO-Pd nanoparticles in a hydroxyl-group functionalized ionic liquid: synthesis, characterization and catalytic performance. Catal Sci Technol 5:1683–1692

Zhang J, Wang J, Fu Y, Zhang B, Xie Z (2015b) Sonochemistry-synthesized CuO nanoparticles as an anode interfacial material for efficient and stable polymer solar cells. RSC Adv 5:28786–28793

Zhang C, Yang Z, Jin W, Wang X, Zhang Y, Zhu S, Yu X, Hu G, Hong Q (2017) Degradation of methomyl by the combination of *Aminobacter* sp. MDW-2 and *Afipia* sp. MDW-3. Lett Appl Microbiol 64:289–296

Zhao YQ, Keogh C, Tony MA (2009) On the necessity of sludge conditioning with non-organic polymer: AOP approach. J Res Sci Technol 6(3):151–155

Zhong X, Barbier J, Duprez D, Zhang H, Royer S (2012a) Modulating the copper oxide morphology and accessibility by using micro-/mesoporous SBA-15 structures as host support: effect on the activity for the CWPO of phenol reaction. Appl Catal B 122:123–134

Zhong X, Barbier J, Duperz D, Zhang H, Royer S (2012b) Modulating the copper oxide morphology and accessibility by using micro-/mesoporous SBA-15 structures as host support: effect on the activity for the CWPO of phenol reaction. Appl Catal B 121:123–134

Zhu HT, Zhang CY, Yin YS (2004) Rapid synthesis of copper nanoparticles by sodium hypophosphite reduction in ethylene glycol under microwave irradiation. J Cryst Growth 270:722–728